ACS APPLIED MATERIALS & INTERFACES

Research Article

www.acsami.org

# Biosensors Based on Porous Cellulose Nanocrystal–Poly(vinyl Alcohol) Scaffolds

Bastien Schyrr,[†,‡] Stéphanie Pasche,[†] Guy Voirin,[†] Christoph Weder,[‡] Yoan C. Simon,*[,‡] and E. Johan Foster*[,‡]

[†]CSEM Centre Suisse d'Electronique et de Microtechnique SA, Jaquet-Droz 1, CH-2002 Neuchâtel, Switzerland

[‡]Adolphe Merkle Institute, University of Fribourg, Route de l'Ancienne Papeterie, 1723 Marly, Switzerland

Supporting Information

**ABSTRACT:** Cellulose nanocrystals (CNCs), which offer a high aspect ratio, large specific surface area, and large number of reactive surface groups, are well suited for the facile immobilization of high density biological probes. We here report functional high surface area scaffolds based on cellulose nanocrystals (CNCs) and poly(vinyl alcohol) (PVA) and demonstrate that this platform is useful for fluorescence-based sensing schemes. Porous CNC/PVA nanocomposite films with a thickness of 25–70 nm were deposited on glass substrates by dip-coating with an aqueous mixture of the CNCs and PVA, and the porous nanostructure was fixated by heat treatment. In a subsequent step, a portion of the scaffold's hydroxyl surface groups was reacted with 2-(acryloxy)ethyl (3-isocyanato-4-methylphenyl)carbamate to permit the immobilization of thiolated fluorescein-substituted lysine, which was used as a first sensing motif, via nucleophile-based thiol–ene Michael addition. The resulting sensor films exhibit a nearly instantaneous and pronounced change of their fluorescence emission intensity in response to changes in pH. The approach was further extended to the detection of protease activity by immobilizing a Förster-type resonance energy transfer chromophore pair via a labile peptide sequence to the scaffold. This sensing scheme is based on the degradation of the protein linker in the presence of appropriate enzymes, which separate the chromophores and causes a turn-on of the originally quenched fluorescence. Using a standard benchtop spectrometer to monitor the increase in fluorescence intensity, trypsin was detected at a concentration of 250 μg/mL, i.e., in a concentration that is typical for abnormal proteolytic activity in wound fluids.

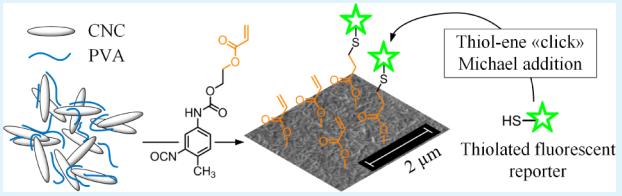


**KEYWORDS:** *cellulose nanocrystals, biosensing, nanocomposites, photodetection, porous scaffold*

## INTRODUCTION

During the past decade, microarray technology has emerged as a powerful tool for genome and proteome analysis,[1,2] high-throughput drug screening,[3,4] and medical diagnostics.[5,6] Lab-on-a-chip devices can provide a rapid, automated, and economical analysis in a miniature format with small quantities of samples. A continued objective of researchers in this field is to improve the signal-to-noise ratio, for example, through the design of sensing platforms that generate amplified responses to analytes. In the case of fluorescence-based transduction schemes, concepts to achieve such amplification include surface plasmon-enhanced fluorescence spectroscopy,[7,8] the use of photonic crystals,[9,10] and amplified fluorescence quenching in conjugated polyelectrolytes.[11,12] An alternative approach is to increase the number of detection sites by creating high-surface-area sensors, which generate stronger signals and also lend themselves to rapid responses.[13,14] High-surface-area sensing materials with a high density of immobilized recognition sites have been prepared in various ways. Illustrative examples include porous films consisting of nanoporous organosilicates,[13] polymer brushes,[15] and nanostructured surfaces prepared, for example, by electrochemical etching of polymer (silicon) films.[14] An interesting alternative is the use of materials that offer an inherently high surface area, such as immobilized carbon nanotubes, electrospun fibers, or $TiO_2$ nanorods.[16]

We show here that cellulose nanocrystals (CNCs), which offer a high aspect ratio, large specific surface area, and large number of reactive surface groups, are well suited for the fabrication of scaffolds for sensing applications. In contrast to carbon nanotubes, whose acute toxicity precludes their utilization *in vivo*,[17] CNCs appear to be rather benign.[18,19] In addition, cellulose's strong hydrophilicity promises reduced nonselective adsorption of biological materials that often causes degradation of transducer surfaces.[20]

CNCs are rod-like, highly crystalline, high-modulus particles that are readily obtained through the controlled acid hydrolysis of cellulosic materials.[21] CNCs can be isolated at a low cost from renewable natural sources such as cotton,[22] wood,[23] banana plants,[24] tunicates,[25] and many other species. They have a typical diameter of 5 to 50 nm and a length of 100 to 3000

Received: May 1, 2014
Accepted: June 23, 2014
Published: June 23, 2014

  

nm, depending on the source and the processing conditions. CNCs have found use in a broad variety of nanomaterials, for example, as a mechanically reinforcing filler in polymer nanocomposites,[26−29] mechanically adaptive[30−32] and light-healable[33] polymer nanocomposites, as well as high-surface-area aerogels.[34,35] CNC-reinforced poly(vinyl alcohol) (PVA) gels have been studied as biodegradable and biocompatible matrices with potential applications in tissue engineering. These materials were prepared in several ways, including repeated freeze−thaw cycles,[36,37] solution casting,[38,39] or electrospinning,[40] affording a wide variety of architectures. Previous work from the authors' group has illustrated the use of CNCs and polymer binder to create porous structures.[41] Due to its excellent film-forming properties and numerous positive interactions through hydroxyl groups, PVA constitutes a good polymer choice for deposition of CNC films. More recently, CNCs have been used for the preparation of sensitive materials for bioimaging or biosensing applications. For example, metallic nanoparticles adsorbed on carboxylated CNCs were prepared for electrochemical detection of DNA hybridization.[42] The CNCs were also used for the immobilization of enzymes,[43,44] or labeled with fluorescent molecules to study cellular uptake.[45−48] Finally, a CNC-based sensor for detection of elastase activity was developed by Edwards et al. based on the immobilization of a fluorogenic peptide.[49]

We here report functional high surface area scaffolds based on CNCs and PVA and demonstrate that this platform is useful for fluorescence-based sensing schemes. Thin porous CNC/PVA nanocomposite films were deposited on glass substrates by dip-coating the substrate with an aqueous mixture of CNCs and PVA and fixating the resulting nanostructures by heat treatment.[50] Depending on the drying conditions, different architectures were obtained, ranging from dense films to highly porous structures. In a subsequent step, a portion of the scaffold's hydroxyl surface groups was reacted with 2-(acryloxy)ethyl (3-isocyanato-4-methylphenyl)carbamate to permit the immobilization of sensor molecules via nucleophile-based thiol−ene Michael addition (Schemes 1 and 2).[51]

**Scheme 1. Synthesis of HEA-TDI**

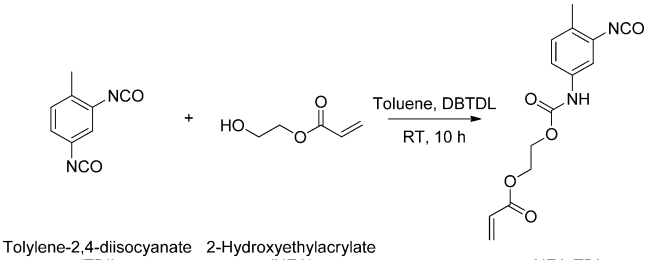


This design offers great versatility because of the possibility to immobilize any thiolated chemical sensing motif on the surface by thiol−ene click chemistry.[52] To demonstrate this, two different sensing schemes were investigated. First, a fluorescein derivative was immobilized on the high surface area films. The resulting enhanced fluorescent signal showed instantaneous response to pH variations, thanks to the porous and hydrophobic nature of the scaffold and a high specific fluorophore content. Second, protease activity detection was demonstrated by tethering a thiolated fluorogenic peptide sequence to the scaffold. Due to their involvement in several diseases or pathologies, such as HIV,[53] different types of cancer,[54] and chronic wounds,[55] the accurate quantification of protease activity is of the utmost interest, which makes the present strategy particularly attractive.

## EXPERIMENTAL SECTION

**Materials.** 2-Propanol puranal grade, sulfuric acid 99.9%, poly(vinyl alcohol) (PVA) 99% hydrolyzed (MW 85 000−124 000), 2-hydroxyethyl acrylate (HEA), tolylene-2,4-diisocyanate (TDI), 10 mM phosphate buffered saline (PBS), PBS containing Tween 20 (PBST), sodium hydroxide pellets puriss p.a. ≥ 98% (NaOH), hydrochloric acid (aqueous, 37%) (HCl), fluorescein sodium salt, hexylamine (HA), tris(2-carboxyethyl)phosphine hydrochloride ≥98% (TCEP), dibutyltin dilaurate 95% (DBTDL), and trypsin-EDTA solution (0.25%, sterile filtered) were purchased from Sigma-Aldrich (Buchs, Switzerland). Hexanes, toluene extra dry, and dimethylformamide (DMF) extra dry over molecular sieves were purchased from Acros Organics (New Jersey, USA). All chemicals were used without further purification, and all aqueous solutions were prepared with deionized water. The thiolated fluorescein-substituted lysine (FL-SH) and fluorogenic peptide (FP-SH) were custom synthesized by the University of Applied Sciences and Arts Western Switzerland (HES-SO, Sion, Switzerland). The peptide design is a modification of the 520 MMP FRET substrate VI from Anaspec (Fremont, USA). The C-terminal quencher QXLTM520 was replaced by a lysine residue that was functionalized with a 4-(4′-dimethylaminophenylazo)benzoic amide (DABCYL) on its side-chain. The peptide was synthesized by solid-phase synthesis with a butanethiol tail introduced at the $NH_2$ terminal upon cleavage from the resin. The model thiolated fluorophore consisted of the thiolated, fluorescein-labeled lysine residue without the rest of the peptide sequence. Cotton-derived cellulose nanocrystals (CNC) were isolated from Whatman filter paper made from cotton linters using sulfuric acid according to known literature procedures.[56,27]

**Preparation of Porous CNC/PVA Nanocomposite Films.** Glass and quartz slides were cleaned by sonication in 2-propanol and rinsed with deionized water. The substrates were then immersed in a bath of concentrated sulfuric acid for 2 min to hydrophilize the surface by revealing the silanol groups on the surface. After surface activation, the substrates were rinsed for 5 min with deionized water and dried with a stream of $N_2$. PVA (5 g) was dissolved in deionized water (500 mL) by heating at 95 °C for 10 h with constant stirring. The PVA solution (10 mg/mL) was then filtered through a cellulose filter (Whatman, Grade 1) and diluted to a PVA content of 1 mg/mL with deionized water. Freeze-dried CNCs were added to reach a concentration of 4 mg/mL, and the mixture was continuously sonicated for 1 h at room temperature in a sonication bath (Bandelin Sonorex Technik RL 70 UH, 40 kHz) to disperse the CNCs. Thin films were deposited onto the clean glass or quartz substrates by dip-coating using a NIMA dip-coater (DC Mono 160) at a speed of 100 mm/min. After deposition, the films were dried under three different conditions to tune their morphology; these included (i) freeze-drying using liquid nitrogen (VirTis BenchTop 2K XL lyophilizer, condenser temperature −78 °C, 25 mT) or (ii) at −20 °C for 2 h in a freezer followed by freeze-drying using liquid nitrogen, and (iii) simple drying under ambient conditions for 2 days. The nanocomposite films were then cured in an oven at 150 °C for 2 h, resulting in insoluble scaffolds (F−OH). Only films dried at room temperature (condition (iii) were used for subsequent derivatization experiments).

The preparation of free-standing films of CNC/PVA nanocomposites was done by mixing PVA (10 mg/mL) with freeze-dried CNCs (40 mg/mL). The mixture was sonicated for 4 h at room temperature and freeze-dried. The resulting free-standing material was cured in an oven at 150 °C for 2 h and employed to visually evaluate the resistance of the nanocomposite to water.

**Synthesis of 2-(Acryloxy)ethyl (3-Isocyanato-4-methylphenyl)carbamate (HEA-TDI).** In an oven-dried 100 mL two-necked round-bottom flask, TDI (17.42 g, 0.1 mol, 10 equiv) was dissolved under nitrogen atmosphere in dry toluene (15 mL), and the solution was cooled to 3 °C. DBTDL (27.5 mg, $4.35 \times 10^{-5}$ mol,

**Scheme 2. Functionalization of Porous CNC/PVA Nanocomposite Films (F−OH) with HEA-TDI**

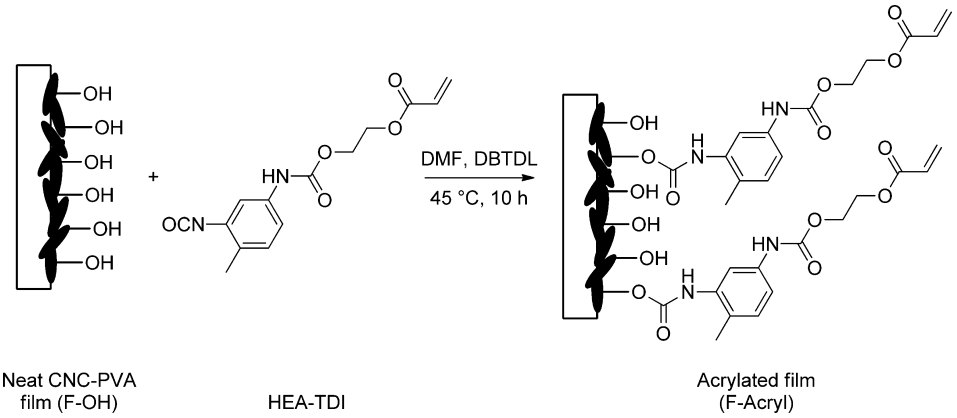


0.004 equiv.) was added and the solution was stirred. Separately, HEA (1.05 mL, 0.01 mol, 1 equiv.) was dissolved in dry toluene (15 mL) and the mixture was added dropwise and under inert conditions to the TDI solution. The homogeneous reaction mixture was stirred for 1 h at 3 °C and allowed to react overnight at room temperature under $N_2$. After the reaction was complete, a white precipitate had formed, which was removed by filtration. The filtrate was precipitated into cold hexanes and the resulting precipitate was washed with hexanes (3 × 100 mL) and dried under reduced pressure at r.t. for 5 h. The title compound was obtained as a white powder with a yield of 56%. $^1$H NMR (300 MHz, DMSO-$d_6$): $\delta$ = 9.8 (s, 1H, C—NH—C), 7.3 (d, 1H, C—CH—C, benzene ring), 7.25−7.0 (m, 2H, C—CH—CH—C, benzene ring), 6.3 (d, 1H, C═$CH_2$), 6.2 (m, 1H, C═$CH_2$), 6.0 (d, 1H, (COO)CH═C), 4.3 (m, 4H, O—$CH_2$—$CH_2$—O), 2.2 (s, 3H, C—$CH_3$).

**Functionalization of the Porous CNC/PVA Nanocomposite Films with HEA-TDI (F-Acryl).** Prior to functionalization, the porous CNC/PVA nanocomposite film on glass or quartz (F−OH) was heated at 120 °C for 1 h in a two-necked 50 mL round-bottom flask. In a separate 25 mL round-bottom flask that had previously been dried at 120 °C for 2 h, HEA-TDI (400 mg, 1.38 mmol) and 3 drops of DBTDL (2.6 mM) were dissolved in dry DMF (10 mL) under $N_2$. This solution was added to the reaction vessel containing the F−OH and the reaction was performed at 45 °C overnight, stirring under $N_2$. The resulting samples with F-Acryl surfaces were subsequently rinsed with DMF (3 × 10 mL) and acetone (10 mL), and subsequently dried and stored under ambient conditions until further use.

The degree of substitution (DS) was approximated from the weight gain of CNCs after their modification with HEA-TDI in solution. We calculated a DS of 0.12 (with respect to the total number of cellulose chains), using previously reported methods,[57] which fell within the previously reported range of isocyanate coupling onto CNCs.[57,58] This value is close to the ratio of surface chains to the total number of chains of 0.19 calculated by Goussé et al.,[59] which suggests that a large fraction of the hydroxyl groups on the CNC surface was reacted.

**Michael Addition of Thiolated Fluorescein-Substituted Lysine (FL-SH) with Acrylated Porous CNC/PVA Nanocomposite Films (F-FL).** The acrylated porous CNC/PVA nanocomposite films (F-Acryl) were cut into pieces with an area of 1 $cm^2$ using a diamond pen. The most efficient functionalization was obtained for the following procedure, which was based on several literature protocols.[51,60,61] A buffer solution was prepared by mixing PBS (10 mM) with SDS (8.1 mM) and HA (1 mM), and the pH was adjusted to 7.4 using 0.1 M HCl. A solution of FL-SH (200 $\mu$L) in DMSO (1 mM) was combined with the buffer solution (1.8 mL) to result a mixed-solvent solution with a FL-SH concentration of 0.1 mM, before TCEP was added until a concentration of 0.05 mM was achieved. The F-Acryl substrates were then immersed in the reaction mixture and allowed to react overnight at 40 °C in 3 mL glass test tubes. The resulting samples with F-FL surfaces were subsequently washed with PBS (3× 10 min) and stored in PBS.

**Michael Addition of Thiolated Fluorogenic Peptide (FP-SH) with Acrylated Porous CNC/PVA Nanocomposite Films (F-FP).** Due to its hydrophobicity, the thiolated fluorogenic peptide (FP-SH) was first dissolved in a 1:1 v/v mixture of acetonitrile and deionized water (1 mM). This solution was further diluted with a solution comprising PBS (10 mM, pH 7.4), SDS (8.1 mM), HA (0.1 mM), and TCEP (0.005 mM). Pieces of the F-Acryl substrates with an area of 1 $cm^2$ were then immersed in the reaction mixture and allowed to react overnight at 40 °C in 3 mL glass test tubes. The resulting samples with F-FP surfaces were subsequently washed 3 times with a 1:1 v/v mixture of acetonitrile and deionized water, followed by deionized water, before they were dried under a stream of $N_2$ and stored in a refrigerator at 4 °C.

**Analytical Methods.** *UV/Vis and Fluorescence Spectroscopy.* UV/vis spectroscopy was used to characterize the optical absorption of porous CNC/PVA nanocomposite films deposited on quartz slides before (F−OH) and after reaction with HEA-TDI (F-Acryl). Absorbance spectra were recorded between 200 and 400 nm using a Shimadzu UV-2401 PC spectrophotometer with a resolution of 1 nm. Fluorescence emission of porous CNC/PVA nanocomposite films modified with the fluorescent sensor molecules (F-FL and F-FP) was measured on a UV/vis plate reader spectrometer (TECAN Infinite PRO), using 24-well plates (BD Biosciences, San Jose, USA). The amount of immobilized fluorophore or fluorogenic peptide was determined after hydrolysis of pieces of the F-FL or F-FP samples with an area of 1 $cm^2$ with NaOH (1 M, 1 mL) at room temperature for 7 and 10 days, respectively. The fluorescence intensity ($\lambda_{exc}$ = 490 nm, $\lambda_{em}$ = 530 nm, gain 90) was compared to standards of the fluorescein-substituted lysine in NaOH (1M, 1 mL) to determine the fluorophore concentration. For enzymatic tests, the functionalized surfaces were cut into 0.5 $cm^2$ samples using a diamond pen and placed inside a 96-well plate. The fluorescence intensity ($\lambda_{exc}$ = 480 nm, $\lambda_{em}$ = 540 nm, gain 100) in PBS (200 $\mu$L) was first measured to generate a baseline. Enzymatic solutions (200 $\mu$L) consisting of trypsin (250 $\mu$g/mL) in PBS were then added to the samples, and fluorescence was monitored every 2 min over the course of 1 h.

*Detection of pH Changes with F-FL.* Light from a 488 nm argon laser (162A-07, Spectra-Physics, Santa Clara, USA) was focused on the sample placed inside a 96-well plate with an incident angle of 45°. A lens was placed normal to the sample to collect the fluorescence previously filtered using a colored filter (OG530, Schott AG, Mainz, Germany) and coupled into a 600 $\mu$m diameter glass optical fiber connected to an avalanche diode (C5460, Hamamatsu Photonics, Hamamatsu, Japan). The fluorescence intensity was recorded with a time lapse of 100 ms. The system comprised a lock-in amplifier (SRS810, Stanford Research Systems Inc., Sunnyvale, USA) connected to a chopper (SR540, Stanford Research Systems Inc.) set at a frequency of 280 Hz for reduction of background noise. For in situ measurements of pH changes, F-FL samples were immersed in tilted position in NaOH (1 M, 50 $\mu$L), before HCl (1M, 100 $\mu$L) was added to the well. Alternatively, the F-FL samples were immersed in HCl (1

M, 50 μL) before adding NaOH (1 M, 100 μL). The sensor response time was calculated as the average time required for 95% of signal variation for three identical experiments. Reference experiments were conducted with 50 μL of a solution of fluorescein in 1 M NaOH (0.08 mM) to which HCl (1 M, 100 μL) was added.

*Contact Angle Measurements.* Static contact angle measurements were performed using a Krüss Drop Shape Analysis system DSA10 on neat porous CNC/PVA nanocomposite films (F−OH) as well as on the modified (F-Acryl) films. For each sample, the contact angle was measured over three different regions by depositing a 5 μL drop of deionized water, and the average angle value was reported.

*Atomic Force Microscopy (AFM).* AFM images of the porous CNC/PVA nanocomposite films (F−OH) deposited on glass slides were acquired on a Nano Wizard II (JPK Instruments) microscope in tapping mode using a silicon cantilever (spring constant 42 N/m, resonance frequency 320 kHz). The coating thickness was determined from scratched samples by measuring the depth profile across the groove.

*Scanning Electron Microscopy (SEM).* The appearance and porosity of porous CNC/PVA nanocomposite films (F−OH) was characterized by SEM (Philips XL30 ESEM-FEG, 5 kV) after deposition of a conductive carbon coating.

*Fourier Transform Infrared Spectroscopy (FTIR).* To monitor the surface modification reaction, FTIR spectra of neat porous CNC/PVA nanocomposite films (F−OH) and the nanocomposites after reaction with HEA-TDI (F-Acryl), both deposited on glass slides at a speed of 100 mm/min, were collected on a PerkinElmer Spectrum 65 spectrometer in ATR mode between 4000 and 600 $cm^{-1}$ with a resolution of 4 $cm^{-1}$ and 16 scans per sample.

*Nuclear Magnetic Resonance Spectroscopy (NMR).* $^1H$ NMR (300 MHz, 200 scans) spectra were recorded in dry deuterated DMSO (DMSO-$d_6$) at room temperature on a Bruker Avance III 300 MHz.

## RESULTS AND DISCUSSION

**Preparation of Porous CNC/PVA Nanocomposite Scaffolds and Functionalization with Acrylate Anchor Groups.** Taking advantage of the CNCs high functionality and aspect ratio, and using them as structuring agent, functional high surface area films were fabricated by dip-coating a mixture of PVA and CNCs. CNCs were extracted from cotton pulp using sulfuric acid treatment. This process introduces a small concentration of sulfate ester groups on the CNC surfaces, which promote good dispersibility in water and other polar solvents on account of electrostatic repulsion.[62] Stable CNC dispersions in an aqueous solution of PVA could thus be obtained by sonication and these mixtures were used to coat glass (and for UV measurements quartz) slides in a dip-coating process. Prior to coating, the substrates were made hydrophilic using sulfuric acid to improve surface wetting by the CNC/PVA mixture, which proved critical for the deposition of high quality films. Due to the high density of hydroxyl groups present on the surfaces of the CNCs and the PVA, favorable hydrogen bonding between the two components is thought to contribute to the deposition of homogeneous films.

Different architectures were obtained by varying the processing conditions, as can be seen from representative scanning electron microscopy (SEM) images (Figure 1). When freeze-dried in liquid nitrogen, a fibrillar structure was obtained with a pore size on the order of 1 to 2 μm (Figure 1a). When the samples were frozen at −20 °C before freeze-drying, smaller pores were obtained with sizes on the order of 0.5 to 1 μm (Figure 1b). In both cases, the resulting CNC/PVA scaffolds showed fractures over the entire surface and were exceedingly difficult to manipulate due to fragility. The structure formation process is driven by the phase separation that occurs as ice crystals form and demix from the polymer, leaving behind a

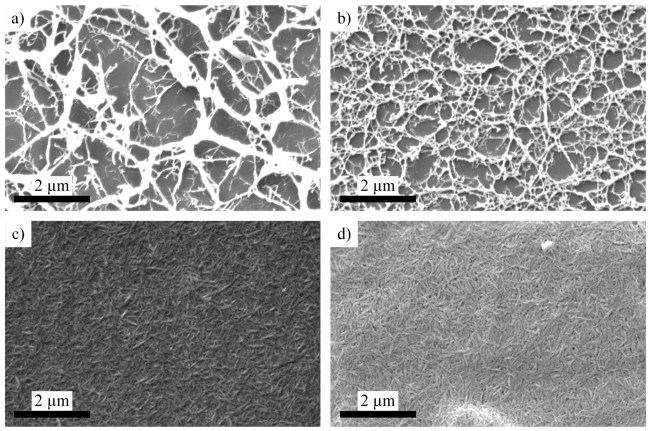


**Figure 1.** Scanning electron micrographs of porous CNC/PVA nanocomposite films deposited by dip-coating glass substrates at a speed of 100 mm/min in an aqueous solution containing 1 mg/mL PVA and 4 mg/mL CNC. (a) Freeze-dried, (b) frozen at −20 °C for 2 h followed by freeze-drying, (c) dried in air at ambient pressure, and (d) dried in air at ambient pressure followed by curing at 150 °C for 2 h.

porous structure upon water removal.[35] Smaller pores were thus obtained when first freezing at −20 °C, because of the smaller ice crystals that formed at this temperature. By contrast, drying at room temperature under normal pressure resulted in homogeneous, stronger, and denser films with much smaller pore size (Figure 1c). Adapting a recently reported annealing step that causes cross-linking of the PVA without the need for any additional chemical cross-linking agent,[31,63,64] the scaffolds produced by ambient drying were cured at 150 °C for 2 h to render them water insoluble. A comparison of Figures 1c and 1d shows that no significant difference in the film morphology can be observed by SEM inspection after thermal treatment.

To assess the water stability after curing, free-standing films of the CNC/PVA nanocomposites prepared by freeze-drying CNC/PVA mixtures were heat-treated at 150 °C and immersed in water for 4 days at 40 °C without any visible degradation of the material. The thickness of the CNC/PVA nanocomposite scaffolds could be tuned between 25 and 70 nm by varying the deposition speed in the range of 25−200 mm/min, as shown by AFM measurements of samples produced under room conditions (Supporting Figure S1).

The surface modification of cellulose, and particularly CNCs, has been performed by many methods, including grafting with isocyanate or acyl chloride, oxidation, and silylation.[65] For the grafting of biological moieties or sensing molecules such as fluorophores, a three-step reaction is typically employed. The first two steps involve derivatization of the CNC surface with amino groups, followed by reaction with isocyanate[47,66,46] or succinimidyl ester.[49] For example, Nielsen et al. performed esterification of the CNC surface with methacrylic acid for thiol−ene addition of cysteamine.[47] Dong et al. started with decoration of CNCs using epichlorhydrin.[46] Alternatively, the modification of CNCs has been achieved in a single step using isothyocyanate derivatives of fluorescein and rhodamine,[47] or using 5-(4,6-dichlorotriazinyl)aminofluorescein (DTAF).[45] Thiol−ene chemistry has become an attractive tool in polymer science, as it permits the connection of (macro)molecules under mild reaction conditions, has a high tolerance to the presence of oxygen and water, and offers high coupling efficiency.[52] It has found many applications in controlled

**Scheme 3. Michael Addition Reaction Used to Immobilize Sensor Molecules on Acrylate-Functionalized Porous CNC/PVA Nanocomposite Films**

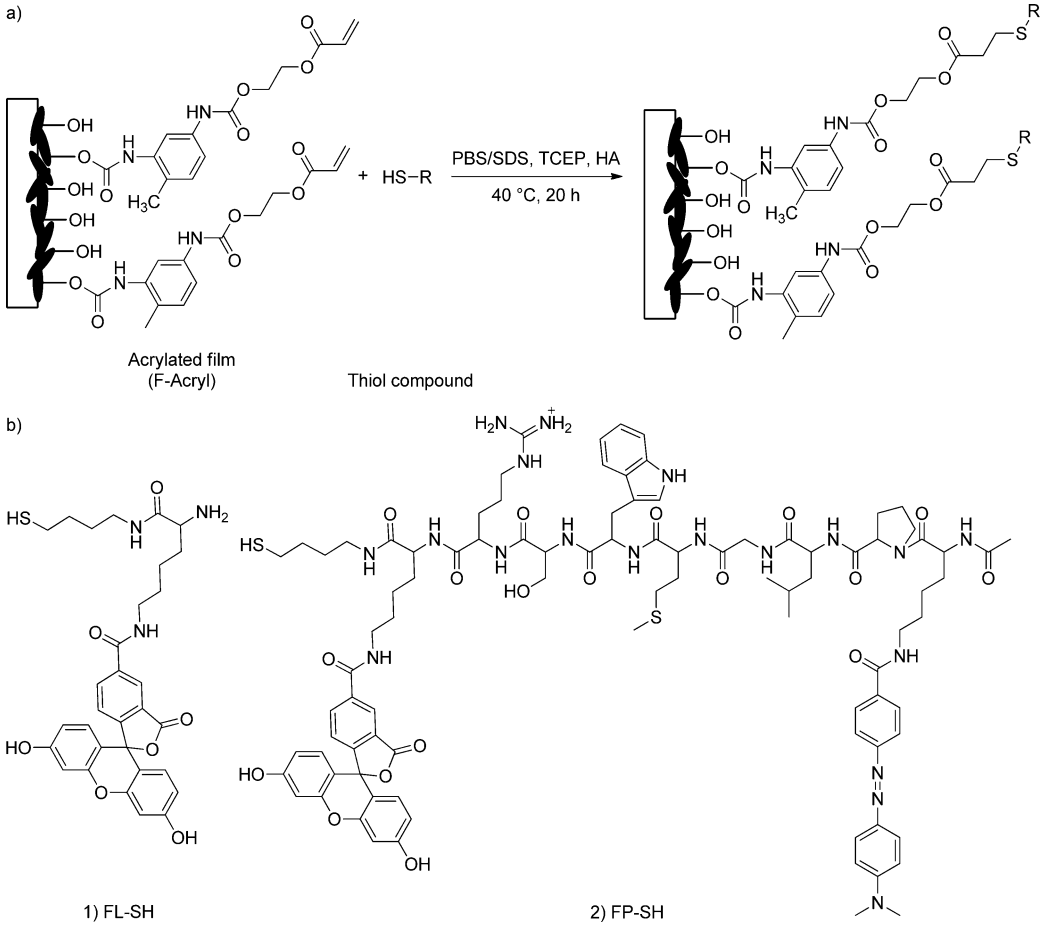


surface grafting,[67,68] polymer functionalization,[69,70] protein immobilization,[71] and hydrogels and biomaterials.[72−74] In order to utilize this framework to covalently attach sensor molecules of choice to the porous CNC/PVA nanocomposite scaffolds, the films were equipped with acrylate anchor groups. Thus, 2-(acryloxy)ethyl (3-isocyanato-4-methylphenyl)-carbamate (HEA-TDI) was prepared using isocyanate chemistry according to a known literature procedure with minor modifications (Scheme 1).[75] The procedure consists of reacting HEA hydroxyl groups with 10-fold excess of the diisocyanate compound TDI in the presence of a catalyst to obtain the monoadduct HEA-TDI, which retains the second isocyanate function for grafting onto the CNCs. Indeed, isocyanate chemistry has been successfully used for the direct modification of CNCs surface hydroxyl groups,[57,58] achieving a high degree of surface grafting through a stable urethane moiety.[57]

Infrared spectroscopy confirmed the disappearance of hydroxyl groups in the region between 3200 and 3600 $cm^{-1}$ and the formation of the urethane bond at 3340 $cm^{-1}$ (N−HCOO group). A remaining isocyanate functionality was still present, as confirmed by the strong peak at 2265 $cm^{-1}$. Heat-treated porous CNC/PVA nanocomposite films (F−OH) were dried at 120 °C to avoid side reactions between the HEA-TDI and residual water, and subsequently reacted with HEA-TDI to yield an acrylate-functionalized porous CNC/PVA nanocomposite films (F-Acryl) (Scheme 2). F-Acryl was characterized by UV/vis and FTIR spectroscopy (Figure S4, Supporting Information). The presence of the HEA-TDI residue's aromatic ring was confirmed by the appearance of characteristic UV absorption bands at $\lambda$ = 212, 238, and 286 nm. As a result of limited film thickness (<100 nm), the absorption in the IR region was predominantly due to the glass substrate (Si—O—Si stretching, 1500−600 $cm^{-1}$). However, the FTIR spectrum clearly shows the disappearance of the isocyanate band at 2270 $cm^{-1}$ as well as the appearance of signals corresponding to N—H stretching (3345 $cm^{-1}$), C═O stretching (1720 $cm^{-1}$), and N—H bending (1605 $cm^{-1}$), which all indicate that HEA-TDI was successfully reacted with the substrate. The functionalization of the scaffold with acrylate anchor groups was further reflected by a change in the sessile drop test, giving contact angles from 29.9° ± 3.3 for F—OH to 52.2° ± 1.2 for F-Acryl, which is consistent with a more hydrophobic surface compared to the originally hydroxyl-rich surface.

**Immobilization of Fluorescein on Porous CNC/PVA Nanocomposite Films.** The first sensor molecule explored in this study was fluorescein, a fluorescent molecule whose emission characteristics are pH-dependent, and which has been widely employed in sensing applications.[76,77] To produce fluorescein-decorated porous CNC/PVA nanocomposite films (F-FL), thiolated fluorescein-substituted lysine (FL-SH) was reacted with F-Acryl under nucleophile-catalyzed Michael addition reaction conditions (Scheme 3). Because the reaction is greatly influenced by the polarity and pH of the reaction medium,[78] the reaction conditions (solvents, reaction times, temperature, and catalysts) were varied to maximize attach-

ment. To assess coupling efficiency, F-FL samples produced under the various conditions were subsequently immersed in 1 M aqueous sodium hydroxide for 1 week to hydrolytically cleave the fluorescein from the surface and the concentration of the released dye was monitored via the fluorescence of the supernatant solution. Although this procedure induced film degradation, a model experiment dismissed any influence of dissolved PVA on the fluorescein emission properties (Figure S5, Supporting Information). The amount of fluorescein immobilized under the different reaction conditions was thus determined, using a comparison with reference solutions of fluorescein in the same solvent and assuming complete hydrolysis (Figure S6, Supporting Information). This analysis revealed a maximum immobilized fluorescein density of 96 pmol/cm$^2$ when using phosphate buffered saline with sodium dodecyl sulfide as a surfactant, in the presence of TCEP and HA as catalysts and conducting the reaction at a temperature of 40 °C for 20 h. In PBS, F-FL samples showed a 5-fold higher fluorescence emission intensity compared to PVA-only films functionalized under the same conditions, which shows the improvement of the nanostructured surface over a flat nonporous substrate (PVA).

**pH-Sensing with Fluorescein-Grafted Porous CNC/PVA Nanocomposite Films.** The porous nature and large specific surface area of the CNC/PVA nanocomposite scaffolds not only permit the immobilization of a high density of sensor molecules but should also enable rapid transport of analytes to the sensing sites. Although the thin nature of the films did not allow direct measurement of specific surface area by BET methods, the sensing rates suggested high available areas. To confirm this, the fluorescein-grafted porous CNC/PVA nanocomposite films were used as pH sensors and their response was compared to that of a solution comprising the same chromophore. Figure 2 shows the changes of the fluorescence intensity that occurred when HCl was added to a solution of NaOH (starting pH 14, final pH 0.5) containing either the new solid-state sensor or, as a reference, the unbound sensor molecule in the dissolved state. The change in fluorescence intensity was almost instantaneous in both cases. In the case of the solid-state sensors, 95% of the reduction of the signal intensity was reached after 1.24 ± 0.45 s. An identical switching speed was observed (1.16 ± 0.26 s) upon switching from acidic to basic pH. Gratifyingly, the switching speed of the solid-state sensor based on the fluorescein-grafted porous CNC/PVA nanocomposite is identical with that recorded for the reference solution of fluorescein (1.0 ± 0.1 s). Although this result suggests that in the present experiment the response time is in both cases limited by mixing step and does not capture the kinetics of quenching, the data clearly indicate that the new sensor platform enables rapid and reliable sensing of simple analytes in an aqueous environment.

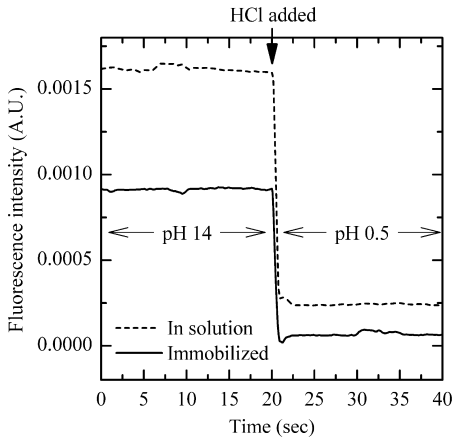


**Figure 2.** Change of the fluorescence intensity (monitored at 530 nm) upon addition of 2 equiv. of 1 M HCl to a 1 M NaOH solution containing the sensor. The pH change was initiated at time $t$ = 20 s. Shown are the responses of the new fluorescein-grafted porous CNC/PVA nanocomposite films (immobilized, solid line) and a reference solution (in solution, dashed line) of fluorescein sodium salt dissolved in 1 M NaOH.

**Application of Porous CNC/PVA Nanocomposite Films for Protease Detection.** Building on the successful proof-of-concept for pH-sensing with fluorescein-grafted porous CNC/PVA nanocomposite films, the acrylated scaffold was modified with a more complex sensing motif to detect enzyme activity. This was achieved by immobilizing a specific fluorogenic peptide (FP-SH) sequence (Scheme 3). Few studies have reported the immobilization of peptides on CNCs.[49,79] Barazzouk et al. employed oxidized CNCs to couple *N*-ethyl-*N*′-(3-(dimethylamino)propyl)carbodiimide hydrochloride, and formed an active ester upon reaction with *N*-hydroxysuccinimide for coupling with amino groups on peptides.[79] Edwards et al. prepared glycine-modified CNCs for coupling of a succinyl-bearing peptide sequence.[49] They used this system for in situ detection of elastase activity in chronic wounds.

Detecting enzymatic activity is of great interest due to the role of proteases in several pathologies such as chronic wounds,[80] where elevated and persistent activity is linked to the uncontrolled degradation of the extracellular matrix components that promote healing. Several studies have shown the implication of these high protease levels and approaches to address it.[81] Being able to monitor efficiently their activity is thus highly important for diagnostic purpose as well as evaluate the effect of protease activity reduction treatments.[82,83] In clinical settings, protease detection actually relies on swab sample analysis using the tedious but very sensitive gel zymography technique, or based on solution fluorescence assay using fluorogenic peptides.

The principle of the sensing scheme using the fluorogenic peptide is as follows: in the immobilized state, a specific peptide sequence links the fluorophore (5-carboxyfluorescein) with DABCYL, which serves as a quencher such that the fluorescence of the fluorophore is suppressed through Förster resonance energy transfer (FRET) to the quencher.[84] Upon cleavage of the peptide sequence by a protease, the quencher is released, while the 5-carboxyfluorescein remains immobilized on the scaffold, and the fluorescence is turned on. Thus, the presence of the protease can be sensed by monitoring the increase of the emission intensity of the sensor system.

To functionalize the porous CNC/PVA nanocomposite scaffolds with the fluorogenic peptide (FP-SH), the latter was designed to feature a butanethiol connector to facilitate nucleophile-catalyzed Michael addition as reported for the pH-sensing FL-SH reported above. The reaction was again conducted at 40 °C in a mixture of PBS/SDS, HA, and TCEP. The catalyst concentrations were decreased to a tenth in comparison to the reaction conditions employed for the immobilization of FL-SH in order to minimize the risk of side reactions such as aza-Michael addition that have been observed for long reaction times and large excess of catalyst.[60,85] We

observed comparable fluorescence emission intensities at 540 nm when F-Acryl surfaces were functionalized with FL-SH using both catalyst concentrations, suggesting that the reaction yield remained comparable (Table S1, Supporting Information). Immobilized peptide densities were measured in solution after hydrolysis of F-FP films in NaOH and comparison with solutions of F-SH standards in NaOH. Densities of 13, 21, 23, and 28 pmol/cm$^2$ were measured for reaction times of 1, 2, 4, and 24 h respectively, indicating that the reaction was essentially complete after 2 h and that the level of functionalization compares favorably with previously described flat surfaces.[86−88] For instance, Fixe et al. reported a maximal density of 12 ± 0.8 pmol/cm$^2$ of single stranded 18-oligonucleotides DNA (ssDNA) immobilized on flat aminated PMMA surfaces modified with glutaraldehyde.[86] Houseman et al. realized a microarray using Diels−Alder-mediated immobilization of a peptide−cyclopentadiene conjugate onto a benzoquinone-derivatized surface, reaching a peptide density of 10 pmol/cm$^2$.[87] Wegner et al. measured a surface coverage of 25 pmol/cm$^2$ using a disulfide exchange reaction between a cysteine-modified peptides and a self-assembled monolayer on gold.[88] To confirm the functionalization of the acrylated porous CNC/PVA nanocomposite films with FP-SH, contact angles were measured and an increase from 52.2° ± 1.2 for F-Acryl to 67.4° ± 1.3 after 24 h reaction was observed, consistent with the attachment of lypophilic FP-SH.

The enzyme-sensing ability of the new sensor was probed using trypsin as a model analyte. The fluorogenic peptide-grafted porous CNC/PVA nanocomposite films prepared under different conditions (resulting in different peptide densities) were immersed into PBS solution containing trypsin at a concentration of 250 μg/mL (Figure 3). This concentration is within the range of protease levels found in chronic wounds fluids.[80] The emission intensity−time traces shown in Figure 3 show that the fluorescence intensity increases over the course of 1 h and the observed intensity increases with the density of immobilized fluorogenic peptide; however, sensor materials with a peptide density of 23 and 28 pmol/cm$^2$ displayed a similar behavior in the presence of 250 μg/mL trypsin, suggesting that a saturation level has been reached. Although the distribution in CNC morphology can influence signal measurement, such artifacts are averaged by the testing procedure that involves relatively large (0.5 × 0.5 cm) samples, and an instrument excitation light spot diameter of 0.3 mm. No change of the fluorescence intensity was observed in the absence of the enzyme, which confirms that the sensor system, at least in the time frame investigated here, is robust and shown no hydrolytic degradation. The system also did not show a response when exposed to a solution containing trypsin at a concentration of 20 μg/mL, which puts a lower end to the detection limit of the enzymatic sensors investigated here.

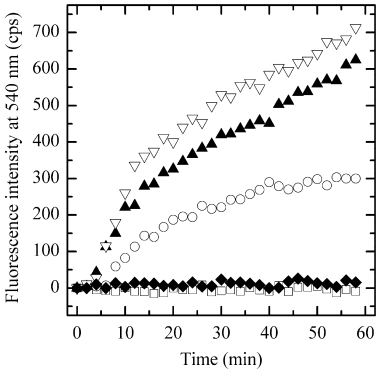


**Figure 3.** Evolution of the fluorescence emission intensity at 540 nm of porous CNC/PVA nanocomposite films derivatized with a fluorogenic protein (F-FP), upon exposure to trypsin in PBS (250 μg/mL). The density of the fluorogenic peptide immobilized on the scaffold was varied via the reaction time used for the immobilization. (○) 13 pmol fluorogenic peptide/cm$^2$ (1 h reaction time); (▲) 23 pmol fluorogenic peptide/cm$^2$ (4 h reaction time); (▽) 28 pmol fluorogenic peptide/cm$^2$ (24 h reaction time). The data for the highest density substrate (28 pmol/cm$^2$) exposed to (♦) 20 μg/mL trypsin in PBS and (□) neat PBS are also shown. Fluorescence emission was measured in counts per second (cps).

The covalent attachment of the fluorophore on the sensor surface was probed after the enzymatic test. Following exposure to trypsin, the substrate was further cleaned by washing with a 1:1 solution of ACN:deionized water for 1 min, and the fluorescence emission was monitored again in PBS. No significant differences were observed after washing, which confirms that the increase in fluorescence intensity results from cleavage of surface-bound peptides and cannot be imparted to detached peptides because of ester bond hydrolysis or retroaddition reaction.

## CONCLUSIONS

In summary, we have shown that CNC/PVA nanocomposites can be readily be processed into robust, water-insoluble high-surface-area scaffolds by dip-coating, and appropriate drying and annealing steps. On account of the large number of surface hydroxyl groups made available by both the CNCs and the PVA, these scaffolds could readily be derivatized with acrylate functions, which permit the subsequent introduction of a high concentration of fluorescent sensor motifs by thiol−ene Michael addition reactions. The reaction conditions used for the immobilization are mild and tolerant, so that the sensing motif can be selected virtually at will. pH sensors made by immobilization of fluorescein display a robust and extremely rapid response to pH changes. These characteristics benefit from the availability of a large number of surface-bound fluorophores and the hydrophilic nature and the porosity of the scaffold. To probe a more complex design, the approach was further extended to the detection of protease activity by immobilizing a Förster-type resonance energy transfer chromophore pair via a labile peptide sequence to the scaffold. Using a standard benchtop spectrometer to monitor the increase in fluorescence intensity, trypsin was detected at a concentration that is typical for abnormal proteolytic activity. Taken together, the results presented here support the conclusion that the porous CNC/PVA nanocomposites are a versatile scaffold for the development of new biosensors for applications in wound diagnosis and other biomedical applications.

## ASSOCIATED CONTENT

### Supporting Information

Topographic AFM images and trace height measurements of CNC/PVA (F−OH) films deposited at various dip-coater withdrawal speeds and dried at room conditions; UV and FTIR measurements of HEA-TDI, F−OH film and F-acryl film; FL-SH fluorescence emission calibration curve; experimental table for Michael addition reactions. This material is available free of charge via the Internet at http://pubs.acs.org.

## AUTHOR INFORMATION


### Corresponding Authors

*Y. C. Simon. E-mail: yoan.simon@unifr.ch.

*E. J. Foster. E-mail: johan.foster@unifr.ch.


### Notes

The authors declare no competing financial interest.

## ACKNOWLEDGMENTS

The authors gratefully acknowledge financial support from the Swiss National Science Foundation (NRP 62: Smart Materials, Nr. 406240_126046), the Nano-Tera initiative (project TecInTex), and the Adolphe Merkle Foundation. We also acknowledge Silvana Mueller for help with the film preparation and Tobias Kuhnt for useful discussion and great support with synthesis steps, as well as Dr. Bernard Wenger for valuable support with fluorescence change kinetic measurements.

## REFERENCES


(1) Kononen, J.; Bubendorf, L.; Kallionimeni, A.; Bärlund, M.; Schraml, P.; Leighton, S.; Torhorst, J.; Mihatsch, M. J.; Sauter, G.; Kallionimeni, O.-P. Tissue Microarrays for High-Throughput Molecular Profiling of Tumor Specimens. *Nat. Med.* **1998**, *4*, 844−847.

(2) MacBeath, G.; Schreiber, S. L. Printing Proteins as Microarrays for High-Throughput Function Determination. *Science* **2000**, *289*, 1760−1763.

(3) Debouck, C.; Goodfellow, P. N. DNA Microarrays in Drug Discovery and Development. *Nat. Genet.* **1999**, *21*, 48−50.

(4) Ma, H.; Horiuchi, K. Y. Chemical Microarray: A New Tool for Drug Screening and Discovery. *Drug Discovery Today* **2006**, *11*, 661−668.

(5) Walter, G.; Büssow, K.; Lueking, A.; Glökler, J. High-Throughput Protein Arrays: Prospects for Molecular Diagnostics. *Trends Mol. Med.* **2002**, *8*, 250−253.

(6) Rusling, J. F.; Kumar, C. V.; Gutkind, J. S.; Patel, V. Measurement of Biomarker Proteins for Point-of-Care Early Detection and Monitoring of Cancer. *Analyst* **2010**, *135*, 2496.

(7) Steele, J. M.; Gagnidze, I.; Wiele, S. M. Efficient Extraction of Fluorescence Emission Utilizing Multiple Surface Plasmon Modes from Gold Wire Gratings. *Plasmonics* **2010**, *5*, 319−324.

(8) Hung, Y.-J.; Smolyaninov, I. I.; Davis, C. C.; Wu, H.-C. Fluorescence Enhancement by Surface Gratings. *Opt. Express* **2006**, *14*, 10825.

(9) Zhang, Y.-Q.; Wang, J.-X.; Ji, Z.-Y.; Hu, W.-P.; Jiang, L.; Song, Y.-L.; Zhu, D.-B. Solid-State Fluorescence Enhancement of Organic Dyes by Photonic Crystals. *J. Mater. Chem.* **2006**, *17*, 90.

(10) Zhang, W.; Cunningham, B. T. Fluorescence Enhancement by a Photonic Crystal with a Nanorod-Structured High Index Layer. *Appl. Phys. Lett.* **2008**, *93*, 133115.

(11) Thomas, S. W.; Joly, G. D.; Swager, T. M. Chemical Sensors Based on Amplifying Fluorescent Conjugated Polymers. *Chem. Rev.* **2007**, *107*, 1339−1386.

(12) Pinto, M. R. Amplified Fluorescence Sensing of Protease Activity with Conjugated Polyelectrolytes. *Proc. Natl. Acad. Sci. U. S. A.* **2004**, *101*, 7505−7510.

(13) Harris, B. C.; Korampally, V.; Weilbaecher, C.; Polo-Parada, L.; Grant, S.; Gangopadhyay, S. Protease Biosensing on Novel High Surface Area Organosilicate Nanoporous Films. *Sens. Actuators, B* **2013**, *176*, 351−359.

(14) Rossi, A. M.; Wang, L.; Reipa, V.; Murphy, T. E. Porous Silicon Biosensor for Detection of Viruses. *Biosens. Bioelectron.* **2007**, *23*, 741−745.

(15) Barbey, R.; Kauffmann, E.; Ehrat, M.; Klok, H.-A. Protein Microarrays Based on Polymer Brushes Prepared via Surface-Initiated Atom Transfer Radical Polymerization. *Biomacromolecules* **2010**, *11*, 3467−3479.

(16) Zhang, W.; Ganesh, N.; Block, I. D.; Cunningham, B. T. High Sensitivity Photonic Crystal Biosensor Incorporating Nanorod Structures for Enhanced Surface Area. *Sens. Actuators, B* **2008**, *131*, 279−284.

(17) Lam, C.-w.; James, J. T.; McCluskey, R.; Arepalli, S.; Hunter, R. L. A Review of Carbon Nanotube Toxicity and Assessment of Potential Occupational and Environmental Health Risks. *Crit. Rev. Toxicol.* **2006**, *36*, 189−217.

(18) Clift, M. J. D.; Foster, E. J.; Vanhecke, D.; Studer, D.; Wick, P.; Gehr, P.; Rothen-Rutishauser, B.; Weder, C. Investigating the Interaction of Cellulose Nanofibers Derived from Cotton with a Sophisticated 3D Human Lung Cell Coculture. *Biomacromolecules* **2011**, *12*, 3666−3673.

(19) Dong, S.; Hirani, A. A.; Colacino, K. R.; Lee, Y. W.; Roman, M. Cytotoxicity and Cellular Uptake of Cellulose Nanocrystals. *Nano LIFE* **2012**, *02*, 1241006.

(20) Edwards, J. V.; Prevost, N.; French, A.; Concha, M.; DeLucca, A.; Wu, Q. Nanocellulose-Based Biosensors: Design, Preparation, and Activity of Peptide-Linked Cotton Cellulose Nanocrystals Having Fluorimetric and Colorimetric Elastase Detection Sensitivity. *Engineering* **2013**, *05*, 20−28.

(21) Camarero Espinosa, S.; Kuhnt, T.; Foster, E. J.; Weder, C. Isolation of Thermally Stable Cellulose Nanocrystals by Phosphoric Acid Hydrolysis. *Biomacromolecules* **2013**, *14*, 1223−1230.

(22) Kumar, S.; Hofmann, M.; Steinmann, B.; Foster, E. J.; Weder, C. Reinforcement of Stereolithographic Resins for Rapid Prototyping with Cellulose Nanocrystals. *ACS Appl. Mater. Interfaces* **2012**, *4*, 5399−5407.

(23) Azizi Samir, M. A. S.; Alloin, F.; Dufresne, A. Review of Recent Research into Cellulosic Whiskers, Their Properties and Their Application in Nanocomposite Field. *Biomacromolecules* **2005**, *6*, 612−626.

(24) Mueller, S.; Weder, C.; Foster, E. J. Isolation of Cellulose Nanocrystals from Pseudostems of Banana Plants. *RSC Adv.* **2013**, *4*, 907.

(25) Marchessault, R. H.; Morehead, F. F.; Walter, N. M. Liquid Crystal Systems from Fibrillar Polysaccharides. *Nature* **1959**, *184*, 632−633.

(26) Favier, V.; Chanzy, H.; Cavaille, J. Y. Polymer Nanocomposites Reinforced by Cellulose Whiskers. *Macromolecules* **1995**, *28*, 6365−6367.

(27) Capadona, J. R.; van den Berg, O.; Capadona, L. A.; Schroeter, M.; Rowan, S. J.; Tyler, D. J.; Weder, C. A Versatile Approach for the Processing of Polymer Nanocomposites with Self-Assembled Nanofibre Templates. *Nat. Nanotechnol.* **2007**, *2*, 765−769.

(28) Eichhorn, S. J.; Dufresne, A.; Aranguren, M.; Marcovich, N. E.; Capadona, J. R.; Rowan, S. J.; Weder, C.; Thielemans, W.; Roman, M.; Renneckar, S.; Gindl, W.; Veigel, S.; Keckes, J.; Yano, H.; Abe, K.; Nogi, M.; Nakagaito, A. N.; Mangalam, A.; Simonsen, J.; Benight, A. S.; Bismarck, A.; Berglund, L. A.; Peijs, T. Review: Current International Research into Cellulose Nanofibres and Nanocomposites. *J. Mater. Sci.* **2010**, *45*, 1−33.

(29) Schroers, M.; Kokil, A.; Weder, C. Solid Polymer Electrolytes Based on Nanocomposites of Ethylene Oxide-Epichlorohydrin Copolymers and Cellulose Whiskers. *J. Appl. Polym. Sci.* **2004**, *93*, 2883−2888.

(30) Shanmuganathan, K.; Capadona, J. R.; Rowan, S. J.; Weder, C. Stimuli-Responsive Mechanically Adaptive Polymer Nanocomposites. *ACS Appl. Mater. Interfaces* **2010**, *2*, 165−174.

(31) Jorfi, M.; Roberts, M. N.; Foster, E. J.; Weder, C. Physiologically Responsive, Mechanically Adaptive Bio-Nanocomposites for Biomedical Applications. *ACS Appl. Mater. Interfaces* **2013**, *5*, 1517−1526.

(32) Annamalai, P. K.; Dagnon, K. L.; Monemian, S.; Foster, E. J.; Rowan, S. J.; Weder, C. Water-Responsive Mechanically Adaptive Nanocomposites based on Styrene-Butadiene Rubber and Cellulose Nanocrystals - Processing Matters. *ACS Appl. Mater. Interfaces* **2013**, *6*, 967−976.

(33) Coulibaly, S.; Roulin, A.; Balog, S.; Biyani, M. V.; Foster, E. J.; Rowan, S. J.; Fiore, G. L.; Weder, C. Reinforcement of Optically Healable Supramolecular Polymers with Cellulose Nanocrystals. *Macromolecules* **2013**, *47*, 152−160.

(34) Korhonen, J. T.; Kettunen, M.; Ras, R. H. A.; Ikkala, O. Hydrophobic Nanocellulose Aerogels as Floating, Sustainable, Reusable, and Recyclable Oil Absorbents. *ACS Appl. Mater. Interfaces* **2011**, *3*, 1813−1816.
(35) Gawryla, M. D.; van den Berg, O.; Weder, C.; Schiraldi, D. A. Clay Aerogel/Cellulose Whisker Nanocomposites: A Nanoscale Wattle and Daub. *J. Mater. Chem.* **2009**, *19*, 2118.
(36) Abitbol, T.; Johnstone, T.; Quinn, T. M.; Gray, D. G. Reinforcement with Cellulose Nanocrystals of Poly(vinyl Alcohol) Hydrogels Prepared by Cyclic Freezing and Thawing. *Soft Matter* **2011**, *7*, 2373.
(37) Wang, Y.; Chang, C.; Zhang, L. Effects of Freezing/Thawing Cycles and Cellulose Nanowhiskers on Structure and Properties of Biocompatible Starch/PVA Sponges. *Macromol. Mater. Eng.* **2009**, *295*, 137−145.
(38) Cheng, Q.; Wang, S.; Rials, T. G. Poly(vinyl Alcohol) Nanocomposites Reinforced with Cellulose Fibrils Isolated by High Intensity Ultrasonication. *Composites, Part A* **2009**, *40*, 218−224.
(39) Roohani, M.; Habibi, Y.; Belgacem, N. M.; Ebrahim, G.; Karimi, A. N.; Dufresne, A. Cellulose Whiskers Reinforced Polyvinyl Alcohol Copolymers Nanocomposites. *Eur. Polym. J.* **2008**, *44*, 2489−2498.
(40) Peresin, M. S.; Habibi, Y.; Zoppe, J. O.; Pawlak, J. J.; Rojas, O. J. Nanofiber Composites of Polyvinyl Alcohol and Cellulose Nanocrystals: Manufacture and Characterization. *Biomacromolecules* **2010**, *11*, 674−681.
(41) Mueller, S.; Weder, C.; Foster, E. J. Water-Insoluble Aerogels Made from Cellulose Nanocrystals and Poly(vinyl Alcohol). Submitted.
(42) Liu, H.; Wang, D.; Song, Z.; Shang, S. Preparation of Silver Nanoparticles on Cellulose Nanocrystals and the Application in Electrochemical Detection of DNA Hybridization. *Cellulose* **2011**, *18*, 67−74.
(43) Edwards, J. V.; Prevost, N. T.; Condon, B.; French, A.; Wu, Q. Immobilization of Lysozyme-Cellulose Amide-Linked Conjugates on Cellulose I and II Cotton Nanocrystalline Preparations. *Cellulose* **2012**, *19*, 495−506.
(44) Incani, V.; Danumah, C.; Boluk, Y. Nanocomposites of Nanocrystalline Cellulose for Enzyme Immobilization. *Cellulose* **2013**, *20*, 191−200.
(45) Abitbol, T.; Palermo, A.; Moran-Mirabal, J. M.; Cranston, E. D. Fluorescent Labeling and Characterization of Cellulose Nanocrystals with Varying Charge Contents. *Biomacromolecules* **2013**, *14*, 3278−3284.
(46) Dong, S.; Roman, M. Fluorescently Labeled Cellulose Nanocrystals for Bioimaging Applications. *J. Am. Chem. Soc.* **2007**, *129*, 13810−13811.
(47) Nielsen, L. J.; Eyley, S.; Thielemans, W.; Aylott, J. W. Dual Fluorescent Labelling of Cellulose Nanocrystals for pH Sensing. *Chem. Commun.* **2010**, *46*, 8929.
(48) Hassan, M. L.; Moorefield, C. M.; Elbatal, H. S.; Newkome, G. R.; Modarelli, D. A.; Romano, N. C. Fluorescent Cellulose Nanocrystals via Supramolecular Assembly of Terpyridine-Modified Cellulose Nanocrystals and Terpyridine-Modified Perylene. *Mater. Sci. Eng., B* **2012**, *177*, 350−358.
(49) Edwards, J. V.; Prevost, N.; Sethumadhavan, K.; Ullah, A.; Condon, B. Peptide Conjugated Cellulose Nanocrystals with Sensitive Human Neutrophil Elastase Sensor Activity. *Cellulose* **2013**, *20*, 1223−1235.
(50) Sriupayo, J.; Supaphol, P.; Blackwell, J.; Rujiravanit, R. Preparation and Characterization of $\alpha$-chitin Whisker-Reinforced Poly(vinyl Alcohol) Nanocomposite Films with or without Heat Treatment. *Polymer.* **2005**, *46*, 5637−5644.
(51) Chan, J. W.; Hoyle, C. E.; Lowe, A. B.; Bowman, M. Nucleophile-Initiated Thiol-Michael Reactions: Effect of Organocatalyst, Thiol, and Ene. *Macromolecules* **2010**, *43*, 6381−6388.
(52) Dondoni, A. The Emergence of Thiol-Ene Coupling as a Click Process for Materials and Bioorganic Chemistry. *Angew. Chem., Int. Ed.* **2008**, *47*, 8995−8997.
(53) Kohl, N. E.; Emini, E. A.; Schleif, W. A.; Davis, L. J.; Heimbach, J. C.; Dixon, R. A.; Scolnick, E. M.; Sigal, I. S. Active Human Immunodeficiency Virus Protease is Required for Viral Infectivity. *Proc. Natl. Acad. Sci. U. S. A.* **1988**, *85*, 4686−4690.
(54) Egeblad, M.; Werb, Z. New Functions for the Matrix Metalloproteinases in Cancer Progression. *Nat. Rev. Cancer.* **2002**, *2*, 161−174.
(55) Wysocki, A. Wound Fluids and the Pathogenesis of Chronic Wounds. *J. Wound Ostomy Continence Nurs.* **1996**, *23*, 283−290.
(56) Dong, X. M.; Revol, J.-F.; Gray, D. G. Effect of Microcrystallite Preparation Conditions on the Formation of Colloid Crystals of Cellulose. *Cellulose* **1998**, *5*, 19−32.
(57) Biyani, M. V.; Foster, E. J.; Weder, C. Light-Healable Supramolecular Nanocomposites Based on Modified Cellulose Nanocrystals. *ACS Macro Lett.* **2013**, *2*, 236−240.
(58) Siqueira, G.; Bras, J.; Dufresne, A. New Process of Chemical Grafting of Cellulose Nanoparticles with a Long Chain Isocyanate. *Langmuir.* **2010**, *26*, 402−411.
(59) Goussé, C.; Chanzy, H.; Excoffier, G.; Soubeyrand, L.; Fleury, E. Stable Suspensions of Partially Silylated Cellulose Whiskers Dispersed in Organic Solvents. *Polymer* **2002**, *43*, 2645−2651.
(60) Li, G.-Z.; Randev, R. K.; Soeriyadi, A. H.; Rees, G.; Boyer, C.; Tong, Z.; Davis, T. P.; Becer, C. R.; Haddleton, D. M. Investigation into Thiol-(Meth)acrylate Michael Addition Reactions Using Amine and Phosphine Catalysts. *Polym. Chem.* **2010**, *1*, 1196.
(61) Firouzabadi, H.; Iranpoor, N.; Jafari, A. A. Micellar Solution of Sodium Dodecyl Sulfate (SDS) Catalyzes Facile Michael Addition of Amines and Thiols to a,b-Unsaturated Ketones in Water under Neutral Conditions. *Adv. Synth. Catal.* **2005**, *347*, 655−661.
(62) van den Berg, O.; Capadona, J. R.; Weder, C. Preparation of Homogeneous Dispersions of Tunicate Cellulose Whiskers in Organic Solvents. *Biomacromolecules* **2007**, *8*, 1353−1357.
(63) Byron, P. R.; Dalby, R. N. Effects of Heat Treatment on the Permeability of Polyvinyl Alcohol Films to a Hydrophilic Solute. *J. Pharm. Sci.* **1987**, *76*, 65−67.
(64) Liu, R. X.; Liu, T. Q.; Zhao, N. Study on Stabilized of Poly(vinyl Alcohol) Nanofibers Based Sandwich Structure Purification Material. *Adv. Mater. Res.* **2012**, *535*−*537*, 473−476.
(65) Lam, E.; Male, K. B.; Chong, J. H.; Leung, A. C.; Luong, J. H. Applications of Functionalized and Nanoparticle-Modified Nanocrystalline Cellulose. *Trends Biotechnol.* **2012**, *30*, 283−290.
(66) Mahmoud, K. A.; Mena, J. A.; Male, K. B.; Hrapovic, S.; Kamen, A.; Luong, J. H. Effect of Surface Charge on the Cellular Uptake and Cytotoxicity of Fluorescent Labeled Cellulose Nanocrystals. *ACS Appl. Mater. Interfaces* **2010**, *2*, 2924−2932.
(67) Goldmann, A. S.; Barner, L.; Kaupp, M.; Vogt, A. P.; Barner-Kowollik, C. Orthogonal Ligation to Spherical Polymeric Microparticles: Modular Approaches for Surface Tailoring. *Prog. Polym. Sci.* **2012**, *37*, 975−984.
(68) Khire, V. S.; Lee, T. Y.; Bowman, C. N. Surface Modification Using Thiol−Acrylate Conjugate Addition Reactions. *Macromolecules* **2007**, *40*, 5669−5677.
(69) Pauloehrl, T.; Delaittre, G.; Bastmeyer, M.; Barner-Kowollik, C. Ambient Temperature Polymer Modification by In Situ Phototriggered Deprotection and Thiol−Ene Chemistry. *Polym. Chem.* **2012**, *3*, 1740.
(70) Delaittre, G.; Pauloehrl, T.; Bastmeyer, M.; Barner-Kowollik, C. Acrylamide-Based Copolymers Bearing Photoreleasable Thiols for Subsequent Thiol−Ene Functionalization. *Macromolecules* **2012**, *45*, 1792−1802.
(71) Gupta, N.; Lin, B. F.; Campos, L. M.; Dimitriou, M. D.; Hikita, S. T.; Treat, N. D.; Tirrell, M. V.; Clegg, D. O.; Kramer, E. J.; Hawker, C. J. A Versatile Approach to High-Throughput Microarrays Using Thiol-Ene Chemistry. *Nat. Chem.* **2009**, *2*, 138−145.
(72) Salinas, C. N.; Anseth, K. S. Mixed Mode Thiol−Acrylate Photopolymerizations for the Synthesis of PEG−Peptide Hydrogels. *Macromolecules* **2008**, *41*, 6019−6026.
(73) Lutolf, M. P.; Hubbell, J. A. Synthesis and Physicochemical Characterization of End-Linked Poly(ethylene Glycol)-co-Peptide

Hydrogels Formed by Michael-Type Addition. *Biomacromolecules* **2003**, *4*, 713−722.
(74) Fairbanks, B. D.; Schwartz, M. P.; Halevi, A. E.; Nuttelman, C. R.; Bowman, C. N.; Anseth, K. S. A Versatile Synthetic Extracellular Matrix Mimic via Thiol-Norbornene Photopolymerization. *Adv. Mater.* **2009**, *21*, 5005−5010.
(75) Peng, Z.; Chen, F. Synthesis and Properties of Temperature-Sensitive Hydrogel Based on Hydroxyethyl Cellulose. *Int. J. Polym. Mater.* **2010**, *59*, 450−461.
(76) Klonis, N.; Sawyer, W. H. Spectral Properties of the Prototropic Forms of Fluorescein in Aqueous Solution. *J. Fluoresc.* **1996**, *6*, 147−157.
(77) Sjöback, R.; Nygren, J.; Kubista, M. Absorption and Fluorescence Properties of Fluorescein. *Spectrochim. Acta, Part A* **1995**, *51*, L7−L21.
(78) Mather, B. D.; Viswanathan, K.; Miller, K. M.; Long, T. E. Michael Addition Reactions in Macromolecular Design for Emerging Technologies. *Prog. Polym. Sci.* **2006**, *31*, 487−531.
(79) Barazzouk, S.; Daneault, C. Amino Acid and Peptide Immobilization on Oxidized Nanocellulose: Spectroscopic Characterization. *Nanomaterials* **2012**, *2*, 187−205.
(80) Trengove, N. J.; Stacey, M. C.; Macauley, S.; Bennett, N.; Gibson, J.; Burslem, F.; Murphy, G.; Schultz, G. Analysis of the Acute and Chronic Wound Environments: The Role of Proteases and their Inhibitors. *Wound Repair Regen.* **1999**, *7*, 442−452.
(81) Diegelmann, R. F.; Evans, M. C. Wound Healing: An Overview of Acute, Fibrotic and Delayed Healing. *Front. Biosci., Landmark Ed.* **2004**, *9*, 283−289.
(82) Snyder, R. J.; Driver, V.; Fife, C. E.; Lantis, J.; Peirce, B.; Serena, T.; Weir, D. Using a Diagnostic Tool to Identify Elevated Protease Activity Levels in Chronic and Stalled Wounds: A Consensus Panel Discussion. *Ostomy Wound Manage.* **2011**, *57*, 36−46.
(83) Dargaville, T. R.; Farrugia, B. L.; Broadbent, J. A.; Pace, S.; Upton, Z.; Voelcker, N. H. Sensors and Imaging for Wound Healing: A Review. *Biosens. Bioelectron.* **2013**, *41*, 30−42.
(84) Tokmina-Roszyk, M.; Tokmina-Roszyk, D.; Fields, G. B. The Synthesis and Application of Fmoc-Lys(5-Fam) Building Blocks. *Biopolymers.* **2013**, *100*, 347−355.
(85) Jones, M. W.; Mantovani, G.; Ryan, S. M.; Wang, X.; Brayden, D. J.; Haddleton, D. M. Phosphine-Mediated One-Pot Thiol-Ene "Click" Approach to Polymer-Protein Conjugates. *Chem. Commun.* **2009**, 5272.
(86) Fixe, F. Functionalization of Poly(methyl Methacrylate) (PMMA) as a Substrate for DNA Microarrays. *Nucleic Acids Res.* **2004**, *32*, e9.
(87) Houseman, B. T.; Huh, J. H.; Kron, S. J.; Mrksich, M. Peptide Chips for the Quantitative Evaluation of Protein Kinase Activity. *Nat. Biotechnol.* **2002**, *20*, 270−274.
(88) Wegner, G. J.; Lee, H. J.; Corn, R. M. Characterization and Optimization of Peptide Arrays for the Study of Epitope−Antibody Interactions Using Surface Plasmon Resonance Imaging. *Anal. Chem.* **2002**, *74*, 5161−5168.